A different approach for calculating Franck–Condon factors including anharmonicity

Josep M. Luis[a)]
*Department of Chemistry and Biochemistry, University of California, Santa Barbara, California 93106
and Department of Chemistry, University of Ottawa, Ottawa, Canada K1N 6N5*

David M. Bishop
Department of Chemistry, University of Ottawa, Ottawa, Canada K1N 6N5

Bernard Kirtman
Department of Chemistry and Biochemistry, University of California, Santa Barbara, California 93106

An efficient new procedure for calculating Franck–Condon factors, based on the direct solution of an appropriate set of simultaneous equations, is presented. Both Duschinsky rotations and anharmonicity are included, the latter by means of second-order perturbation theory. The critical truncation of basis set is accomplished by a build-up procedure that simultaneously removes negligible vibrational states. A successful test is carried out on ClO_2 for which there are experimental data and other theoretical calculations. © *2004 American Institute of Physics.*
[DOI: 10.1063/1.1630566]

I. INTRODUCTION

Along with the development of experimental high-resolution vibronic spectroscopies, the problem of analyzing the observed spectra is receiving increased attention. In the Born–Oppenheimer approximation the leading term that governs the spectral intensity pattern is given by the square of the vibrational overlap integrals, also known as Franck–Condon factors (FCF's), between the initial and final states. If the vibrational normal coordinates for the two electronic states are parallel (i.e., if they are the same except for the shift in equilibrium geometry), then these integrals will separate in the harmonic oscillator approximation into a product of individual oscillator terms. In general, however, this is not the case and, discounting possible simplifications due to symmetry, one must evaluate $3N$-6 (or $3N$-5 for linear molecules) dimensional overlap integrals. The difficulty of doing so is compounded by the fact that the difference in equilibrium geometry as well as the anharmonicity of the electronic potential-energy surfaces must be taken into account.

A variety of methods have been proposed for dealing with this problem, particularly at the harmonic level.[1] One of these is based on the generating function approach of Sharp and Rosenstock,[2] which is an extension of the method introduced by Hutchisson[3] for diatomics. This method has been further developed by Chen[4] and improved by Ervin *et al.*[5] in their application to the naphthyl radical. Very recently, Kikuchi *et al.*[6] derived a simpler form of the Sharp and Rosenstock general formula and applied it to SO_2 in the harmonic oscillator approximation. Another method based on the generating function approach is due to Ruhoff[7] who derived recursion relations for the calculation of multidimen-

sional FCF's by generalizing Lermé's[8] procedure for two-dimensional FCF's. Also employing the generating function method, Islampour *et al.* derived a closed-form multidimensional harmonic oscillator expression, where the FCF's were expressed as sums of products of Hermite polynomials.[9]

An alternative procedure, utilizing the recursion relations of Doctorov, Malkin, and Man'ko,[10] has been employed for a variety of molecules such as phenol,[11,12] anthracene,[13] and pyrazine.[14] In addition, two different methods for calculating the FCF's were developed by Faulkner and Richardson.[15] The central feature of their first method is a linear transformation of the normal coordinates in both the ground and excited electronic states in order to effectively remove the Duschinsky rotations[16] (i.e., the transformation of coordinates from one electronic state to another). This was originally restricted to the case where either the initial or final vibrational wave function is the ground state, but Kulander later removed this restriction.[17,18] The second method of Faulkner and Richardson is based on a perturbation expansion of the vibrational wave functions of the excited electronic state in terms of the ground electronic state vibrational wave functions.[15] Finally, Malmqvist and Forsberg[19] have expressed the FCF matrix as the product of lower triangular and upper triangular matrices which are calculated from recursion formulas.

At this juncture we take note of a very different approach, developed by Segev, Heller, and co-workers,[20,21] based on considering the transitions in phase space. Those phase-space points where the classical Wigner function for the initial state is maximal, subject to a classical energy constraint on the final state, determine propensity rules for the FCF's. These rules, in turn, provide a way of selecting the transitions that have substantial intensity and their FCF's can be estimated by subsequent phase-space integration. The truncation of the vibrational basis is a critical aspect in re-

[a)]Permanent address: Institute of Computational Chemistry and Department of Chemistry, University of Girona, Campus de Montilivi, 17071 Girona, Catalonia, Spain.

    813

ducing the computational effort of any method. Our own prescription for doing this is described in Sec. II D.

Although the procedures mentioned above can, in principle, include vibrational anharmonicity not much attention has been paid to this aspect. Iachello's group has developed a procedure based on the use of Morse oscillators in a novel Lie algebraic scheme.[22–24] More recently Mok *et al.*[25] have proposed an expansion technique that builds on the earlier work of Botschwina and co-workers.[26] However, these methods and other approaches[27–29] to the vibrational anharmonicity problem have only been applied to small molecules or to two-dimensional model potentials.[30] Reimers has also described[31] an approximate method for taking into account the floppy motions of large molecules by means of curvilinear coordinates.

Apart from one-photon absorption (and emission) FCF's figure prominently in two-photon absorption (TPA). The vibrational contribution to nonlinear optical (NLO) properties, including TPA,[32] has occupied the attention of the present authors for some time.[33–36] As far as nonresonant NLO processes are concerned, it is also known that mechanical and electrical anharmonicities of ordinary (as well as floppy) molecules often play a major role.[37] On the basis of very approximate treatments[38–40] it has been suggested that the same is true for resonant processes and in particular for TPA. We have now begun to develop a rigorous theory for vibrational effects in TPA in order to investigate that situation more thoroughly. In the course of doing so, we have come across a simple direct way to evaluate FCF's and it is this new scheme that is presented here. Effects due to: (i) changes in the normal coordinates with electronic state (Duschinsky rotations);[16] (ii) changes in the equilibrium geometry with electronic state; and (iii) mechanical anharmonicities in both electronic states, are all taken into account.

In the next section a general theory, which includes all of the above effects, is formulated. Then, in Sec. III we discuss how the resulting equations are solved along with other computational details. This is followed by an example where our method is used to simulate the He I photoelectron (PE) spectrum of ClO_2, in order to compare with the work of Mok *et al.*[25] Finally, we conclude with a brief discussion of future plans for incorporating this methodology into our treatment of TPA for large conjugated molecules.

II. THEORY

The goal of this section is the derivation of a new analytical procedure to calculate the Franck–Condon factors of polyatomic molecules taking into account both the Duschinsky rotations and the mechanical anharmonicity.

A. General formulation

We denote the vibrational Hamiltonian, wave functions, and energies of the ground electronic state by $\hat{H}^g$, $|\psi_{\nu_g}^g\rangle$, and $E_{\nu_g}^g$ and their counterparts for an electronic excited state by $\hat{H}^e$, $|\psi_{\nu_e}^e\rangle$, and $E_{\nu_e}^e$. Note that "g" refers to the ground electronic state and "e" to an excited electronic state throughout. In either case the molecule is assumed to be nonrotating and

thus the rotational state is suppressed. Then the respective Schrödinger equations for nuclear motion are given by

$$\hat{H}^g|\psi_{\nu_g}^g\rangle = E_{\nu_g}^g|\psi_{\nu_g}^g\rangle, \tag{1}$$

$$\hat{H}^e|\psi_{\nu_e}^e\rangle = E_{\nu_e}^e|\psi_{\nu_e}^e\rangle. \tag{2}$$

Multiplication of Eq. (1) by $\langle\psi_{\nu_e}^e|$ and Eq. (2) by $\langle\psi_{\nu_g}^g|$ leads to

$$\langle\psi_{\nu_e}^e|\hat{H}^g|\psi_{\nu_g}^g\rangle = E_{\nu_g}^g S_{\nu_e\nu_g}, \tag{3}$$

$$\langle\psi_{\nu_g}^g|\hat{H}^e|\psi_{\nu_e}^e\rangle = E_{\nu_e}^e S_{\nu_g\nu_e}, \tag{4}$$

where $S_{\nu_e\nu_g}$ are the Franck–Condon overlap integrals (the wave functions are taken to be real):

$$S_{\nu_e\nu_g} = S_{\nu_g\nu_e} = \langle\psi_{\nu_e}^e|\psi_{\nu_g}^g\rangle = \langle\psi_{\nu_g}^g|\psi_{\nu_e}^e\rangle. \tag{5}$$

Subtraction of Eq. (4) from Eq. (3), and using the Hermitian property of $\hat{H}^g$, gives

$$\langle\psi_{\nu_g}^g|\hat{H}^g-\hat{H}^e|\psi_{\nu_e}^e\rangle = (E_{\nu_g}^g - E_{\nu_e}^e)S_{\nu_g\nu_e}. \tag{6}$$

Since the vibrational eigenfunctions for the excited electronic state ($\psi_{\mu_e}^e$ below) form a complete set, the left-hand side of Eq. (6) can be expressed as

$$\langle\psi_{\nu_g}^g|\hat{H}^g-\hat{H}^e|\psi_{\nu_e}^e\rangle = \sum_{\mu_e} \langle\psi_{\nu_g}^g|\psi_{\mu_e}^e\rangle\langle\psi_{\mu_e}^e|\hat{H}^g-\hat{H}^e|\psi_{\nu_e}^e\rangle$$

$$= \sum_{\mu_e} S_{\nu_g\mu_e}\langle\psi_{\mu_e}^e|\hat{H}^g-\hat{H}^e|\psi_{\nu_e}^e\rangle. \tag{7}$$

Equation (7) contains the entire set of Franck–Condon overlaps between the initial vibrational wave function of the ground electronic state and all final vibrational wave functions of the excited electronic state. This allows us to solve for the entire set of overlap integrals in which we are interested simultaneously. If the vibrational wave functions of the electronic excited state had been expanded in terms of the electronic ground-state vibrational wave functions, then only one of the desired overlaps would be obtained and the process would have to be repeated for each final state. In either event the properties of both the ground and excited electronic states are necessary for the calculations.

Combining Eqs. (6) and (7), while taking into account the fact that the total nuclear kinetic energy operator is the same in both Hamiltonians ($\hat{H}^g = \hat{T} + \hat{V}^g$, $\hat{H}^e = \hat{T} + \hat{V}^e$), one obtains

$$\sum_{\mu_e} S_{\nu_g\mu_e}[\langle\psi_{\mu_e}^e|\hat{V}^g-\hat{V}^e|\psi_{\nu_e}^e\rangle + (E_{\nu_e}^e - E_{\nu_g}^g)\delta_{\mu_e\nu_e}]$$

$$= 0, \ \forall\nu_e, \ \text{and} \ \forall\nu_g, \tag{8}$$

where $\delta_{\mu_e\nu_e}$ is the Kronecker delta.

For a given ν_g, Eq. (8) constitutes an infinite set of homogeneous simultaneous linear equations with an infinite number of unknowns $S_{\nu_g\mu_e}$ (all μ_e). The first step in solving this set of equations is to truncate to a finite set of μ_e and ν_e values. The details of the systematic iterative algorithm used

to select the M equations that survive the truncation are given in the next section. Then after dividing by $S_{\nu_g \lambda_e}$ (λ_e is arbitrary as long as $S_{\nu_g \lambda_e} \neq 0$),

$$\sum_{\mu_e}^{M} r_{\lambda_e}^{\mu_e} [\langle \psi_{\mu_e}^e | \hat{V}^g - \hat{V}^e | \psi_{\nu_e}^e \rangle + (E_{\nu_e}^e - E_{\nu_g}^g) \delta_{\mu_e \nu_e}] = 0,$$

$$\{\nu_e\} = \{\mu_e\}, \ \forall \nu_e, \tag{9}$$

where $r_{\lambda_e}^{\mu_e}$ is the ratio,

$$r_{\lambda_e}^{\mu_e} = S_{\nu_g \mu_e} / S_{\nu_g \lambda_e} \tag{10}$$

(the index ν_g is understood in $r_{\lambda_e}^{\mu_e}$). There are M simultaneous equations in Eq. (9) but only $M-1$ unknown ratios; hence one of these equations is redundant. Any one can be omitted (assuming the remaining set is nonsingular) and our choice is to remove the equation corresponding to $\nu_e = \lambda_e$. In order to obtain $S_{\nu_g \mu_e}$ from the ratios $r_{\lambda_e}^{\mu_e}$ we use the normalization condition,

$$\sum_{\mu_e}^{M} S_{\nu_g \mu_e}^2 = \sum_{\mu_e}^{M} \langle \psi_{\nu_g}^g | \psi_{\mu_e}^e \rangle \langle \psi_{\mu_e}^e | \psi_{\nu_g}^g \rangle = 1, \tag{11}$$

which leads to

$$S_{\nu_g \lambda_e} = 1 \bigg/ \sqrt{\sum_{\mu_e}^{M} (r_{\lambda_e}^{\mu_e})^2}. \tag{12}$$

The remaining $S_{\nu_g \mu_e}$ are obtained from Eq. (10) as $S_{\nu_g \mu_e} = r_{\lambda_e}^{\mu_e} S_{\nu_g \lambda_e}$ ($\mu_e \neq \lambda_e$). Finally, the Franck–Condon factors are given by the square of the corresponding Franck–Condon integrals ($F_{\nu_g \mu_e} = S_{\nu_g \mu_e}^2$).

B. Duschinsky rotations

In general the equilibrium geometry and the potential-energy surface (PES) of the electronic excited and ground states are not the same. Therefore the respective normal coordinates $\mathbf{Q}^e$ and $\mathbf{Q}^g$ are also different. The relationship between the two sets of normal coordinates can be obtained from the corresponding relationship between their mass-weighted Cartesian displacement coordinates and the formulas that connect the normal and Cartesian coordinates. For the mass-weighted Cartesian displacement coordinates we have

$$\mathbf{X}^g = \mathbf{X}^e + \mathbf{R}, \tag{13}$$

where $\mathbf{X}^g$ ($\mathbf{X}^e$) represents the coordinates of the electronic ground (excited) state and $\mathbf{R}$ is the vector (in mass-weighted Cartesians) obtained by subtracting the ground-state equilibrium geometry from that of the excited state. The normal coordinates are related to the mass-weighted Cartesian coordinates by

$$\mathbf{Q}^g = \mathbf{L}^{g^\dagger} \mathbf{X}^g \ \text{ and } \ \mathbf{Q}^e = \mathbf{L}^{e^\dagger} \mathbf{X}^e, \tag{14}$$

where $\mathbf{L}^g$ and $\mathbf{L}^e$ are unitary matrices (see, for example, Ref. 41). Six columns of $\mathbf{L}^g$ and $\mathbf{L}^e$ (or five for linear molecules)

are associated with translations and rotations, while the remainder correspond to the normal vibrations. By combining Eqs. (13) and (14) we find that

$$\mathbf{Q}^g = \mathbf{J} \mathbf{Q}^e + \mathbf{K}, \tag{15}$$

where $\mathbf{J} = \mathbf{L}^{g^\dagger} \mathbf{L}^e$ and $\mathbf{K} = \mathbf{L}^{g^\dagger} \mathbf{R}$. The $\mathbf{J}$ matrix describes the Duschinsky rotation between the normal modes of the ground and excited electronic state, while $\mathbf{K}$ is associated with the change in the normal modes due to the displacement of the equilibrium geometry between the two electronic states.

The effect of the Duschinsky rotation and the equilibrium geometry displacement on the Franck–Condon factors occurs in the potential-energy difference $\hat{V}^g - \hat{V}^e$ in Eq. (9) which, for nonlinear states, is given by

$$\hat{V}^g - \hat{V}^e = V_{Q^g=0}^g - V_{Q^e=0}^e + \frac{1}{2} \sum_{i=1}^{3N-6} \left(\frac{\partial^2 V^g}{\partial (Q_i^g)^2} \right)_{Q^g=0}$$

$$\times \left[K_i^2 + 2K_i \sum_{j=1}^{3N-6} J_{ij} Q_j^e + \sum_{j,k=1}^{3N-6} J_{ij} J_{ik} Q_j^e Q_k^e \right]$$

$$- \frac{1}{2} \sum_{i=1}^{3N-6} \left(\frac{\partial^2 V^e}{\partial (Q_i^e)^2} \right)_{Q^e=0} (Q_i^e)^2 \tag{16}$$

in the harmonic approximation.

C. Mechanical anharmonicity

Mechanical anharmonicity can be included through a perturbation treatment using the harmonic oscillator Hamiltonian as the zeroth-order approximation.[42] An alternative approach is to introduce the anharmonicity by using curvilinear coordinates.[31]

Expanding Eq. (8) in orders of perturbation theory, we find that the first-order equation is

$$\sum_{\mu_e} S_{\nu_g \mu_e}^{(1)} [\langle \psi_{\mu_e}^e | \hat{V}^g - \hat{V}^e | \psi_{\nu_e}^e \rangle + (E_{\nu_e}^e - E_{\nu_g}^g) \delta_{\mu_e \nu_e}]^{(0)}$$

$$+ \sum_{\mu_e} S_{\nu_g \mu_e}^{(0)} [\langle \psi_{\mu_e}^e | \hat{V}^g - \hat{V}^e | \psi_{\nu_e}^e \rangle$$

$$+ (E_{\nu_e}^e - E_{\nu_g}^g) \delta_{\mu_e \nu_e}]^{(1)} = 0, \tag{17}$$

where the superscripts (0) and (1) indicate the order of perturbation theory. The zeroth-order equation is identical to Eq. (8) except that all quantities have a superscript (0). This infinite set of equations is truncated to the same finite set $\{\nu_e\} = \{\mu_e\}$ that is used in the zeroth-order equation. As in previous work[32] we take the cubic terms in V^g and V^e to be first order. In that event, the first-order corrections to $E_{\nu_e}^e$ and $E_{\nu_g}^g$ vanish. On the other hand, the first-order corrections to the terms in which the potential-energy difference occurs in Eq. (17) are given by

$\langle \psi^e_{\mu_e} | \hat{V}^g - \hat{V}^e | \psi^e_{\nu_e} \rangle^{(1)}$

$$= \langle \psi^{e(1)}_{\mu_e} | (\hat{V}^g - \hat{V}^e)^{(0)} | \psi^{e(0)}_{\nu_e} \rangle + \langle \psi^{e(0)}_{\mu_e} | (\hat{V}^g - \hat{V}^e)^{(1)} | \psi^{e(0)}_{\nu_e} \rangle$$

$$+ \langle \psi^{e(0)}_{\mu_e} | (\hat{V}^g - \hat{V}^e)^{(0)} | \psi^{e(1)}_{\nu_e} \rangle, \tag{18}$$

where

$$|\psi^{e(1)}_{\nu_e}\rangle = - \sum_{\mu_e \neq \nu_e}^{M} \frac{\langle \psi^{e(0)}_{\nu_e} | \hat{V}^{e(1)} | \psi^{e(0)}_{\mu_e} \rangle | \psi^{e(0)}_{\mu_e} \rangle}{E^{e(0)}_{\mu_e} - E^{e(0)}_{\nu_e}} \tag{19}$$

and

$$(\hat{V}^g - \hat{V}^e)^{(1)} = \frac{1}{6} \sum_{i,j,k=1}^{3N-6} \left(\frac{\partial^3 V^g}{\partial Q^g_i \partial Q^g_j \partial Q^g_k} \right)_{Q^g=0}$$

$$\times \left[K_i K_j K_k + 3 K_i K_j \sum_{l=1}^{3N-6} J_{kl} Q^e_l \right.$$

$$+ 3 K_i \sum_{l,m=1}^{3N-6} J_{jl} J_{km} Q^e_l Q^e_m$$

$$+ \left. \sum_{l,m,n=1}^{3N-6} J_{il} J_{jm} J_{kn} Q^e_l Q^e_m Q^e_n \right]$$

$$- \frac{1}{6} \sum_{i,j,k=1}^{3N-6} \left(\frac{\partial^3 V^e}{\partial Q^e_i \partial Q^e_j \partial Q^e_k} \right)_{Q^e=0} Q^e_i Q^e_j Q^e_k. \tag{20}$$

The column vector $\mathbf{S}^{(1)}_{\mathbf{v}g}$ with components $S^{(1)}_{\nu_g \mu_e}$, can be written as

$$\mathbf{S}^{(1)}_{\mathbf{v}g} = \mathbf{S}'^{(1)}_{\mathbf{v}g} + \mathbf{S}''^{(1)}_{\mathbf{v}g} = \mathbf{S}'^{(1)}_{\mathbf{v}g} + f \mathbf{S}^{(0)}_{\mathbf{v}g}, \tag{21}$$

where $\mathbf{S}'^{(1)}_{\mathbf{v}g}$ is the component of $\mathbf{S}^{(1)}_{\mathbf{v}g}$ orthogonal to $\mathbf{S}^{(0)}_{\mathbf{v}g}$ and $\mathbf{S}''^{(1)}_{\mathbf{v}g}$ is the component of $\mathbf{S}^{(1)}_{\mathbf{v}g}$ parallel to $\mathbf{S}^{(0)}_{\mathbf{v}g}$. The first term on the left-hand side of Eq. (17) vanishes if we substitute $\mathbf{S}^{(0)}_{\mathbf{v}g}$ for the first-order eigenvector $\mathbf{S}^{(1)}_{\mathbf{v}g}$ [cf. Eq. (8)]. Therefore $\mathbf{S}^{(1)}_{\mathbf{v}g}$ is a solution of Eq. (17) for any arbitrary f. We choose f equal to zero so that $\mathbf{S}^{(1)}_{\mathbf{v}g}$ is orthogonal to $\mathbf{S}^{(0)}_{\mathbf{v}g}$ and thereby satisfies the first-order normalization condition

$$2 \sum_{\mu_e} S^{(1)}_{\nu_g \mu_e} S^{(0)}_{\nu_g \mu_e} = 2 \mathbf{S}^{(1)\dagger}_{\mathbf{v}g} \mathbf{S}^{(0)}_{\mathbf{v}g} = 0. \tag{22}$$

One easy procedure to solve the set of simultaneous equations (17) is to transform to a basis consisting of the vector $\mathbf{S}^{(0)}_{\mathbf{v}g}$ and an arbitrary set of $M-1$ vectors perpendicular to $\mathbf{S}^{(0)}_{\mathbf{v}g}$. Then we only need to solve the reduced set of $M-1$ inhomogeneous equations in the subspace orthogonal to $\mathbf{S}^{(0)}_{\mathbf{v}g}$. Once the solution for $S^{(1)}_{\nu_g \mu_e}$ has been determined, the first-order corrections to the FCF's are found as

$$F^{(1)}_{\nu_g \mu_e} = 2 S^{(0)}_{\nu_g \mu_e} S^{(1)}_{\nu_g \mu_e}. \tag{23}$$

A similar procedure may be followed for the second-order correction which is obtained by solving

$$\sum_{\mu_e}^{M} S'^{(2)}_{\nu_g \mu_e} [\langle \psi^e_{\mu_e} | \hat{V}^g - \hat{V}^e | \psi^e_{\nu_e} \rangle + (E^e_{\nu_e} - E^g_{\nu_g}) \delta_{\mu_e \nu_e}]^{(0)}$$

$$+ \sum_{\mu_e}^{M} S''^{(2)}_{\nu_g \mu_e} [\langle \psi^e_{\mu_e} | \hat{V}^g - \hat{V}^e | \psi^e_{\nu_e} \rangle + (E^e_{\nu_e} - E^g_{\nu_g}) \delta_{\mu_e \nu_e}]^{(0)}$$

$$+ \sum_{\mu_e}^{M} S^{(1)}_{\nu_g \mu_e} [\langle \psi^e_{\mu_e} | \hat{V}^g - \hat{V}^e | \psi^e_{\nu_e} \rangle + (E^e_{\nu_g} - E^g_{\nu_g}) \delta_{\mu_e \nu_e}]^{(1)}$$

$$+ \sum_{\mu_e}^{M} S^{(0)}_{\nu_g \mu_e} [\langle \psi^e_{\mu_e} | \hat{V}^g - \hat{V}^e | \psi^e_{\nu_e} \rangle + (E^e_{\nu_e} - E^g_{\nu_g}) \delta_{\mu_e \nu_e}]^{(2)}$$

$$= 0, \tag{24}$$

where we have written $\mathbf{S}'^{(2)}_{\mathbf{v}g}$ for the component of $\mathbf{S}^{(2)}_{\mathbf{v}g}$ orthogonal to $\mathbf{S}^{(0)}_{\mathbf{v}g}$ and $\mathbf{S}''^{(2)}_{\mathbf{v}g}$ for the component of $\mathbf{S}'^{(2)}_{\mathbf{v}g}$ parallel to $\mathbf{S}^{(0)}_{\mathbf{v}g}$. Again the parallel component is given by $\mathbf{S}''^{(2)}_{\mathbf{v}g} = f \mathbf{S}^{(0)}_{\mathbf{v}g}$ where the multiplicative constant f is chosen to satisfy the normalization condition which, in second-order, is

$$0 = 2 \mathbf{S}^{(2)\dagger}_{\mathbf{v}g} \mathbf{S}^{(0)}_{\mathbf{v}g} + \mathbf{S}^{(1)\dagger}_{\mathbf{v}g} \mathbf{S}^{(1)}_{\mathbf{v}g}$$

$$= 2 \mathbf{S}''^{(2)\dagger}_{\mathbf{v}g} \mathbf{S}^{(0)}_{\mathbf{v}g} + \mathbf{S}^{(1)\dagger}_{\mathbf{v}g} \mathbf{S}^{(1)}_{\mathbf{v}g} = 2 f + \mathbf{S}^{(1)\dagger}_{\mathbf{v}g} \mathbf{S}^{(1)}_{\mathbf{v}g} \tag{25}$$

or

$$f = -0.5 \mathbf{S}^{(1)\dagger}_{\mathbf{v}g} \mathbf{S}^{(1)}_{\mathbf{v}g}. \tag{26}$$

In this case $V^{e(2)}$ and $V^{g(2)}$ contain the quartic terms in the expansion of the vibrational potential in terms of normal coordinates:

$$(\hat{V}^g - \hat{V}^e)^{(2)} = \frac{1}{24} \sum_{i,j,k,l=1}^{3N-6} \left(\frac{\partial^4 V^g}{\partial Q^g_i \partial Q^g_j \partial Q^g_k \partial Q^g_l} \right)_{Q^g=0} \left[K_i K_j K_k K_l + 4 K_i K_j K_k \sum_{m=1}^{3N-6} J_{lm} Q^e_m + 6 K_i K_j \right.$$

$$\times \sum_{m,n=1}^{3N-6} J_{km} J_{ln} Q^e_m Q^e_n + 4 K_i \sum_{m,n,p=1}^{3N-6} J_{jm} J_{kn} J_{lp} Q^e_m Q^e_n Q^e_p$$

$$+ \left. \sum_{m,n,p,q=1}^{3N-6} J_{im} J_{jn} J_{kp} J_{lq} Q^e_m Q^e_n Q^e_p Q^e_q \right] - \frac{1}{24} \sum_{i,j,k,l=1}^{3N-6} \left(\frac{\partial^4 V^e}{\partial Q^e_i \partial Q^e_j \partial Q^e_k \partial Q^e_l} \right)_{Q^e=0} Q^e_i Q^e_j Q^e_k Q^e_l. \tag{27}$$

Then $S_{\mathbf{v}g}^{(2)}$ is obtained by solving Eq. (24) for $S_{\mathbf{v}g}^{\prime(2)}$ in a basis orthogonal to $S_{\mathbf{v}g}^{(0)}$ and adding $S_{\mathbf{v}g}^{\prime\prime(2)}=fS_{\mathbf{v}g}^{(0)}$ with the value of f determined by Eq. (26). Finally, the second-order correction to the Franck–Condon factors is given by

$$F_{\nu_g\mu_g}^{(2)}=2S_{\nu_g\mu_e}^{(0)}S_{\nu_g\mu_e}^{(2)}+S_{\nu_g\mu_e}^{(1)}S_{\nu_g\mu_e}^{(1)}. \tag{28}$$

D. Truncation of the vibrational basis set

It is critical to perform the truncation of the vibrational basis set in a way that is efficient and does not create significant error. Our procedure involves an iterative buildup by increasing the range of vibrational quantum numbers while, simultaneously, removing unimportant states.

We begin by identifying an initial guess for the vibrational state associated with the vertical FC transition to the excited electronic state based on energy and geometry considerations. This gives a starting set of vibrational quantum numbers for all modes. Next, an initial basis set is formed which contains all vibrational wave functions wherein the quantum number for each mode differs by less than two units from the corresponding quantum number in the vertical FC state. Equation (9) is solved in this basis to yield an initial set of FC overlaps $S_{\mathbf{v}g}$. Augmentation of the basis set is, then, carried out iteratively. In each iterative cycle we, simultaneously, increase by one unit the maximum quantum number of all modes where the previous two augmentations produced one or more states that have a non-negligible FC overlap (i.e., an overlap larger than 10^{-6}). An exactly analogous procedure is applied at the same time to the minimum quan-

tum number except, of course, that the minimum cannot be reduced below zero. The next step in the cycle is a screening of the states created in this manner which is based on the difference between the quantum number in each mode and the corresponding quantum number for the FC state. If the sum over modes of the absolute value of these differences for any given state is larger than a threshold value, then that state is removed. The threshold is taken to be the largest difference between the maximum and minimum quantum numbers in any one mode considering all states. Mok et al. employed a similar screening criterion to reduce their basis sets.[25] Using this reduced basis Eq. (9) is solved and a new set of FC overlap integrals $S_{\mathbf{v}g}$ is obtained.

Although the algorithm described above limits the growth of the basis set, the latter still increases in size more rapidly than desired. It turns out, however, that most of the FC overlaps obtained from Eq. (9) are quite small. Therefore the cycle is completed by setting all $S_{\mathbf{v}g}$ smaller than a preset threshold (10^{-6}) equal to zero, and the corresponding states are marked for exclusion in subsequent cycles. They are retained, however, for the purpose of augmentation. This simple procedure drastically reduces the growth of the basis set thereby leading to a major improvement in efficiency. The overall process is converged when a complete cycle leads to no augmentation of the basis set.

We tested our algorithm in several different ways for ClO_2. Thus the calculations were repeated separately with: (i) the FC overlap threshold for expanding the range of quantum numbers systematically decreased from 10^{-4} to 10^{-9},
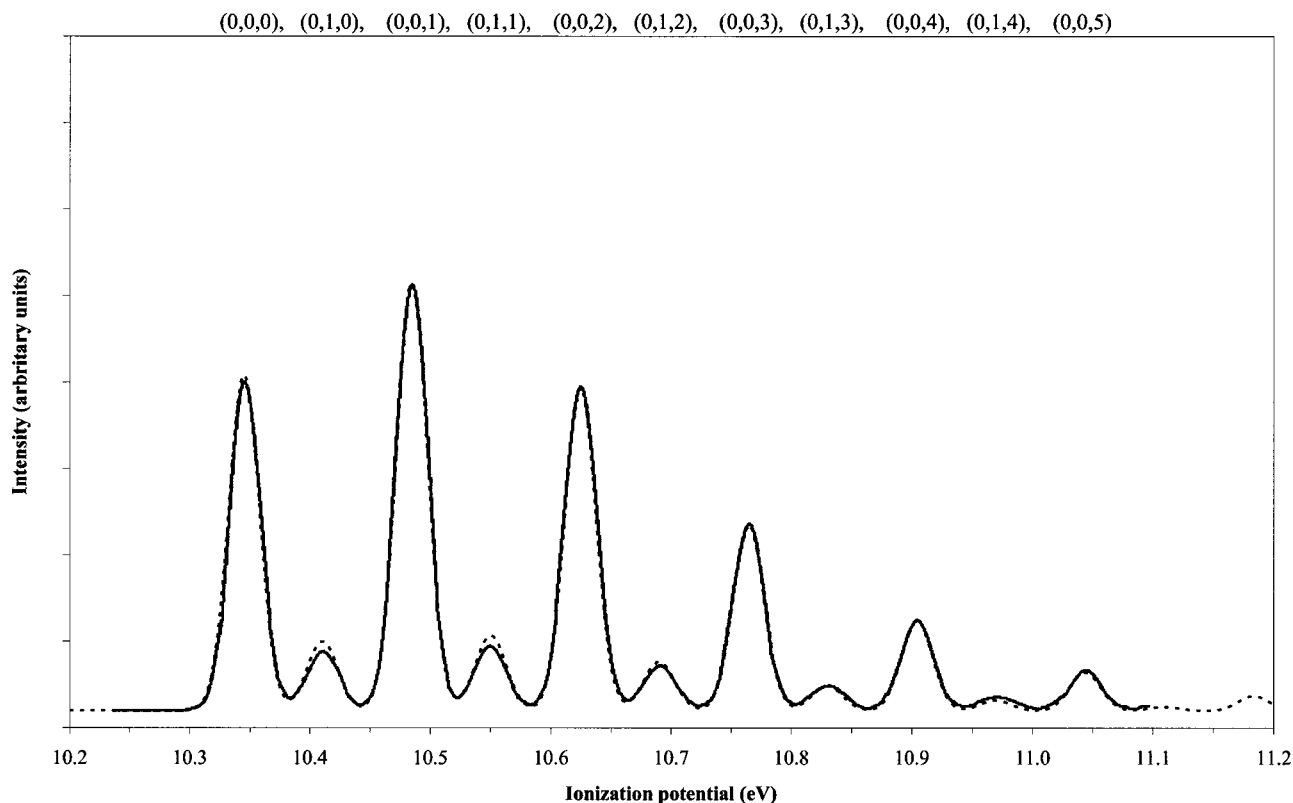

FIG. 1. Simulated first band of the ClO_2 He I PE spectrum using harmonic FCF's obtained from the QCISD PES. The dashed and solid lines represent our work and that of Mok et al. (Ref. 25), respectively. The geometry of ClO_2 is the experimental one (Refs. 51 and 52) and the geometrical parameters of the cation are $R_{Cl-O}=1.410$ Å and $\theta_{O-Cl-O}=121.8°$.

(ii) the FC overlap criterion for excluding states after a complete cycle eliminated, and (iii) the maximum quantum number in each cycle increased by 2 and by 4. Although the test calculations were far more time consuming, the differences in the calculated FCF's were always negligible ($<0.1\%$ for FC overlap). Nevertheless, we realize that our algorithm may need to be further refined when larger systems are considered. As part of our verification strategy we confirmed that the determinant associated with the M simultaneous equations given by Eq. (9) is zero.

III. COMPUTATIONAL DETAILS

In order to test our method we computed the $ClO_2^+ \tilde{X}^1 A_1 \leftarrow ClO_2 \tilde{X}^2 B_1$ ionization band of the He I PE spectrum and compared our results (i) with those of Mok et al.[25] at the same geometries and (ii) with the experimental spectrum obtained by Flesch et al.[43] Harmonic vibrational force constants were obtained numerically from analytical gradients at the quadratic configuration interaction with single and double excitations (QCISD) level, using the GAUSSIAN98 suite of programs.[44] Like Mok et al.,[25] the basis sets 6-311G(2d) and 6-311G(3df) were used to calculate the

neutral and cationic force constants, respectively, for the harmonic calculations. The harmonic and anharmonic force constants derived from the PEF's calculated by Peterson and Werner for the neutral[45] and cationic[46] ground states at the complete active space multi configuration self-consistent field/multi reference configuration interaction (CASSCF/MRCI) level with a cc-pVQZ basis set were used in the anharmonic calculations.

The harmonic vibrational wave function $\psi_{\nu_e}^{e(0)}$ is given by the product of harmonic oscillator functions $\phi_i^{\nu_e}$ for each mode:

$$\psi_{\nu_e}^{e(0)} = \prod_{i=1}^{3N-6} \phi_i^{\nu_e}, \tag{29}$$

and the harmonic vibrational energy is a sum of individual mode contributions. Integrals such as $\langle \psi_{\mu_e}^{e(0)} | (\hat{V}^g - \hat{V}^e)^{(0)} | \psi_{\nu_e}^{e(0)} \rangle$ [cf. Eqs. (9) and (16)] and $\langle \psi_{\nu_e}^{e(0)} | \hat{V}^{e(1)} | \psi_{\mu_e}^{e(0)} \rangle$ [cf. Eq. (19)] can easily be evaluated as a simple product of one-dimensional integrals of the type $\langle \phi_i^{\nu_e} | (Q_i^e)^t | \phi_i^{\mu_e} \rangle$.[32,41] The first- and second-order corrections to the wave function are given by Eq. (19) and[42]

$$|\psi_{\nu_e}^{e(2)}\rangle = \sum_{\alpha_e, \beta_e \neq \nu_e}^{M} \frac{\langle \psi_{\nu_e}^{c(0)} | \hat{V}^{e(1)} | \psi_{\beta_e}^{e(0)} \rangle \langle \psi_{\beta_e}^{e(0)} | \hat{V}^{e(1)} | \psi_{\alpha_e}^{e(0)} \rangle | \psi_{\alpha_e}^{e(0)} \rangle}{(E_{\beta_e}^{e(0)} - E_{\nu_e}^{e(0)})(E_{\alpha_e}^{e(0)} - E_{\nu_e}^{e(0)})} - \sum_{\alpha_e \neq \nu_e}^{M} \frac{\langle \psi_{\nu_e}^{e(0)} | \hat{V}^{e(2)} | \psi_{\alpha_e}^{e(0)} \rangle | \psi_{\alpha_e}^{e(0)} \rangle}{E_{\alpha_e}^{e(0)} - E_{\nu_e}^{e(0)}}$$
$$- \frac{1}{2} \sum_{\alpha_e \neq \nu_e}^{M} \frac{\langle \psi_{\nu_e}^{e(0)} | \hat{V}^{e(1)} | \psi_{\alpha_e}^{e(0)} \rangle^2 | \psi_{\nu_e}^{e(0)} \rangle}{(E_{\alpha_e}^{e(0)} - E_{\nu_e}^{e(0)})^2}, \tag{30}$$

respectively. As mentioned above, the first-order correction to the energy is zero whereas the second-order correction to the energy can be written as

$$E_{\nu_e}^{e(2)} = \langle \psi_{\nu_e}^{e(0)} | \hat{V}^{e(2)} | \psi_{\nu_e}^{e(0)} \rangle - \sum_{\alpha_e \neq \nu_e}^{M} \frac{\langle \psi_{\nu_e}^{e(0)} | \hat{V}^{e(1)} | \psi_{\alpha_e}^{e(0)} \rangle^2}{E_{\alpha_e}^{e(0)} - E_{\nu_e}^{e(0)}}. \tag{31}$$

In order to simulate the spectra we used Gaussian functions with a full width at half maximum of 30 meV. The intensities and positions of the peaks were determined by the theoretical FCF's and vibronic energies, but the positions were uniformly shifted so that the first peak occurs at the experimental adiabatic ionization energy (AIE) of 10.345 eV as measured by Flesch et al.[43]

IV. RESULTS

In Fig. 1 we present our simulated harmonic first band of the ClO_2 He I PE spectrum and the harmonic results of Mok et al. both calculated at the QCISD level. The geometry used was the experimental one[47,48] ($R_{Cl-O} = 1.4698$ Å and $\theta_{O-Cl-O} = 117.41°$) for ClO_2 and that obtained by Mok et al., from an iterative Franck–Condon analysis (IFCA),[49] based on the harmonic result ($R_{Cl-O} = 1.410$ Å and θ_{O-Cl-O}

$= 121.8°$), for the cation. The IFCA procedure consists in adjusting the geometrical parameters systematically until the best match between the simulated and the experimental spectrum is obtained.

Only the two totally symmetric vibrations of ClO_2 are active in the He I PE spectrum and two vibrational progressions related to the symmetric stretching (ν_3) and bending (ν_2) modes are observed. The most intense vibrational progression is composed of the $(0,0,\nu_3)$ peaks, where ν_3 is the quantum number of the symmetric stretch. The second-vibrational progression is formed by the $(0,1,\nu_3)$ peaks. Since the intensities of Mok et al. are in arbitrary units, in order to compare our harmonic spectrum with theirs we forced the intensities of the $(0,0,1)$ peaks to be equal. The comparison shows no appreciable differences in the $(0,0,\nu_3)$ progression, whereas a small discrepancy can be observed for $(0,1,\nu_3)$. This minor discrepancy could be due to differences in the algorithms used to truncate the vibrational basis set. At the harmonic level our theoretical spectrum is essentially the same as that of Mok et al. and thus our geometrical parameters for ClO_2^+, obtained from the best match between the simulated and experimental spectrum, are also the same as theirs.

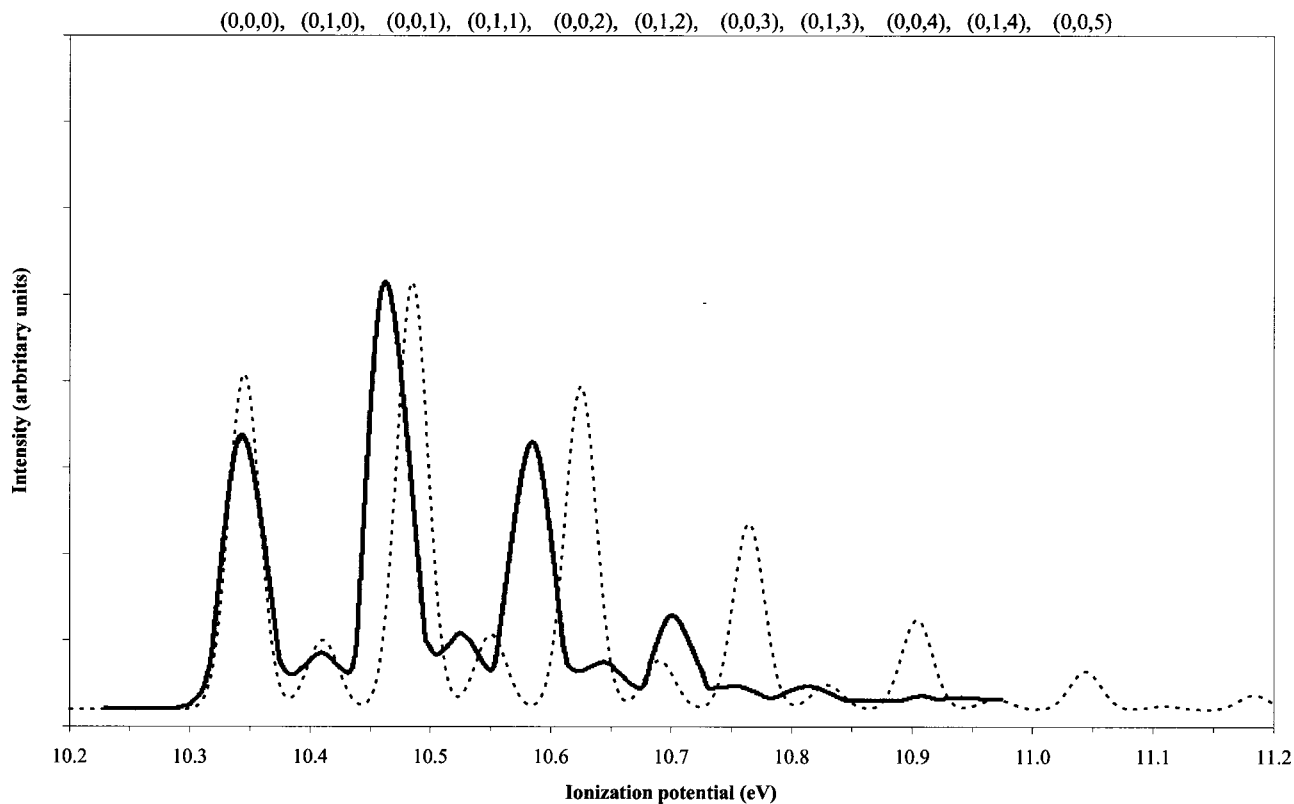Our simulated harmonic and experimental first band of

(0,0,0), (0,1,0), (0,0,1), (0,1,1), (0,0,2), (0,1,2), (0,0,3), (0,1,3), (0,0,4), (0,1,4), (0,0,5)

FIG. 2. Simulated (dashed line) and experimental (Ref. 43) (solid line) first band of the ClO_2 He I PE spectrum. Our theoretical harmonic spectrum is obtained using the OCISD PES. The geometry of ClO_2 is the experimental one (Refs. 51 and 52) and the geometrical parameters of the cation are $R_{Cl-O} = 1.410$ Å and $\theta_{O-Cl-O} = 121.8°$.
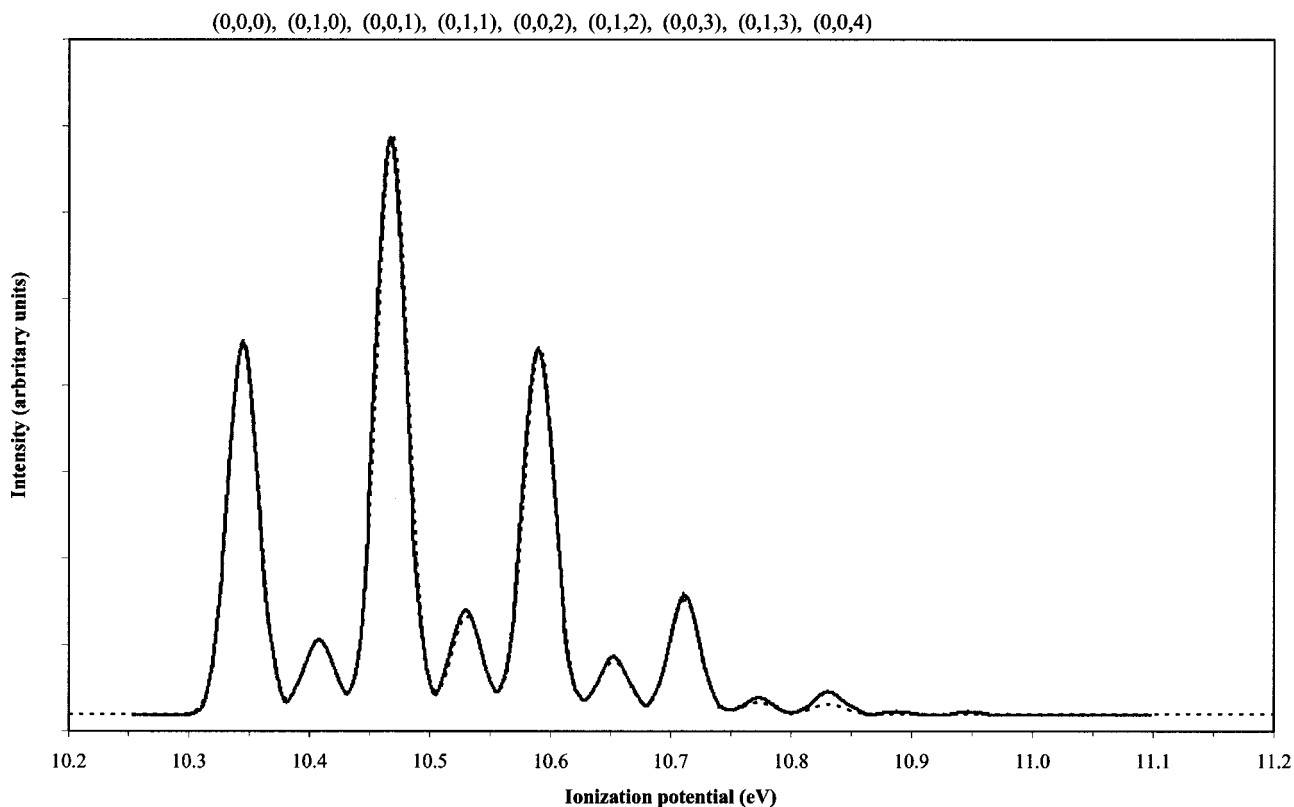
(0,0,0), (0,1,0), (0,0,1), (0,1,1), (0,0,2), (0,1,2), (0,0,3), (0,1,3), (0,0,4)

FIG. 3. Simulated first band of the ClO_2 He I PE spectrum using PEF calculated by Peterson and Werner (Refs. 46 and 47). The dashed and solid lines represent the second-order anharmonic spectra obtained by us and that obtained by Mok *et al.* (Ref. 25), respectively. The geometry of ClO_2 is the experimental one (Refs. 51 and 52) and the geometrical parameters of the cation are $R_{Cl-O} = 1.411$ Å and $\theta_{O-Cl-O} = 121.80$ for our work and $R_{Cl-O} = 1.414$ Å and $\theta_{O-Cl-O} = 121.80$ for Mok *et al.*

(0,0,0), (0,1,0), (0,0,1), (0,1,1), (0,0,2), (0,1,2), (0,0,3), (0,1,3), (0,0,4)
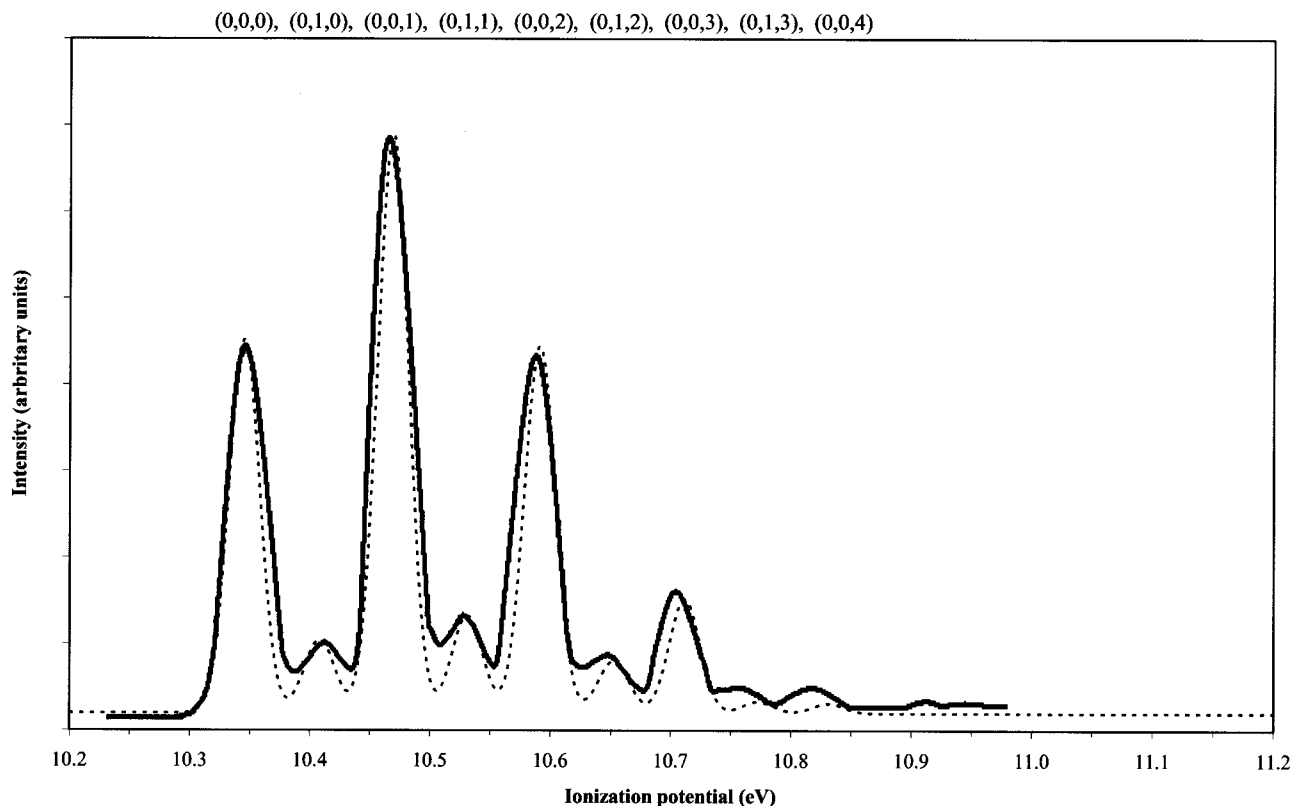

FIG. 4. Simulated (dashed line) and experimental (solid line) first band of the ClO_2 He I PE spectrum. The theoretical second-order anharmonic spectrum is obtained by us using the PEF calculated by Peterson and Werner (Refs. 46 and 47) and the experimental geometry for ClO_2 (Refs. 51 and 52) and R_{Cl-O} = 1.411 Å and θ_{O-Cl-O} = 121.80° as geometrical parameters for the cation.

the He I PE spectrum of ClO_2 determined by Flesch et al.[43] are shown in Fig. 2. Again, in order to compare the two spectra the intensities of the (0,0,1) peaks are forced to be equal. A comparison of the peaks shows two main discrepancies: (i) The intensity ratio between the (0,0,1) peak and the (0,0,0) or (0,0,2) peaks is far larger in the experimental spectrum than in the harmonic simulated spectrum; and (ii) the intensities of the high-energy peaks are much smaller in the experimental spectrum. For instance, whereas the (0,0,5) peak has a intensity similar to the (0,1,2) peak in the harmonic spectrum it is not observed in the experiment.

Mok et al. used a variational method, which involves diagonalization of the Watson Hamiltonian,[50,51] to obtain the anharmonic wave functions as linear combinations of harmonic vibrational wave functions. Then, the FCF's were computed by evaluating harmonic overlap integrals according to Chen's[4] procedure and carrying out a double sum over the harmonic wave functions of both electronic states (see Ref. 25 for details). On the contrary, we include anharmonicity through the application of perturbation theory to Eq. (8). Nevertheless, both methods should give similar results.

The ClO_2^+ equilibrium geometry was obtained by Mok et al. by means of the IFCA procedure using the PEF of Peterson and Werner[45,46] with anharmonicity taken into account. This resulted in R_{Cl-O} = 1.414 Å and θ_{O-Cl-O} = 121.8°. Utilizing the same PEF, and also including anharmonicity, we find that the geometry R_{Cl-O} = 1.411 Å and θ_{O-Cl-O} = 121.8° yields the best agreement with the experi-

mental spectrum. It would be of interest to have an accurate experimental geometry for comparison. In Fig. 3 we present the simulated anharmonic spectra calculated by Mok et al. and ourselves. As in the harmonic case, the intensities of the (0,0,1) peaks were forced to be identical and, then, the theoretical spectra are seen to be very similar. In fact, the only meaningful difference is the intensity of (0,0,4) peak, which is smaller in our spectrum. Including anharmonicity increases the intensity ratio between the (0,0,1) and (0,0,0) or (0,0,2) peaks and also decreases the intensity of the highest energy peaks. Thus, the correction to the harmonic spectrum is in the right direction.

In Fig. 4 we depict the experimental spectrum and our best simulated anharmonic spectrum. It is clear that close similarity between the experimental and simulated spectra cannot be obtained (see Fig. 2) without taking anharmonicity into account. Only the two highest energy peaks [i.e., (0,1,3) and (0,0,4)] show any significant difference from experiment. These differences could be due to anharmonicity contributions higher than second order, which are omitted in our treatment. A comparison of Figs. 2 and 4 reveals the great improvement that is gained by including first- and second-order anharmonicity. Finally, in order to evaluate the convergence of the perturbation theory corrections, we depict in Fig. 5 the first-order anharmonic, and second-order anharmonic simulated spectra. The difference between the first- and second-order results is quite small and, as expected, this
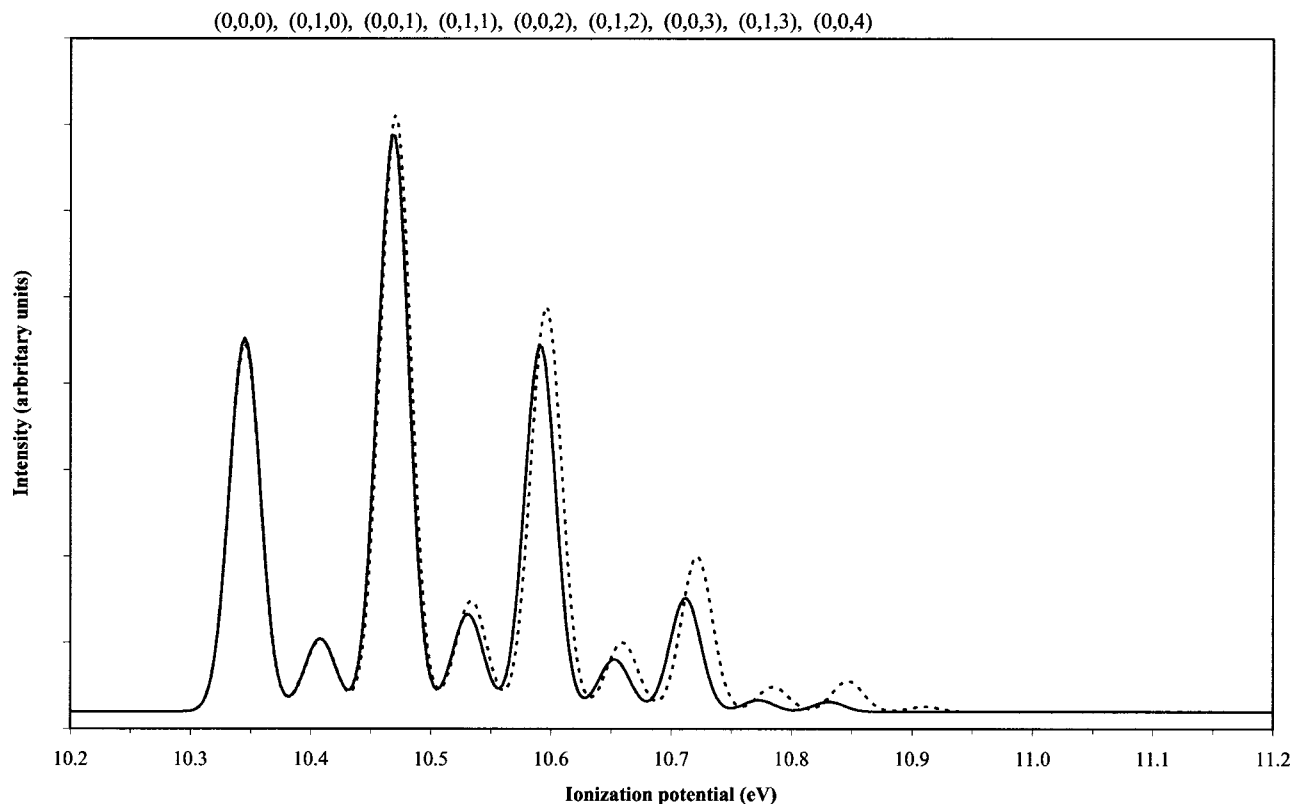
(0,0,0), (0,1,0), (0,0,1), (0,1,1), (0,0,2), (0,1,2), (0,0,3), (0,1,3), (0,0,4)

FIG. 5. Simulated first band of the ClO_2 He I PE spectrum using the PEF calculated by Peterson and Werner (Refs. 46 and 47). The dashed and solid lines represent our first-order and second-order anharmonic spectra, respectively. The geometry of ClO_2 is the experimental one (Refs. 51 and 52) and the geometrical parameters of the cation are $R_{Cl-O} = 1.411$ Å and $\theta_{O-Cl-O} = 121.8°$.

difference increases as the quantum numbers of the cationic state increase.

V. CONCLUSIONS

In this work a new method to calculate FCF's taking into account Duschinsky rotations as well as anharmonicity has been developed and implemented. Harmonic FCF's are obtained in a simple and direct manner by solving a set of homogeneous linear equations [see Eq. (9)]. The Duschinsky rotation and shift of equilibrium geometry appear in the difference potential between the ground and excited electronic states. Anharmonicity is included through a second-order perturbation treatment of the linear equations. The critical truncation of the basis set is carried out through a rapidly convergent procedure whereby the basis set is systematically increased in size while, at the same time, negligible states are removed.

As a verification of our method we have applied it to simulate the first band of the ClO_2 He I PE spectrum. Our harmonic results are in excellent agreement with those of Mok *et al.* who used a different procedure and both calculations predict the same geometry for $ClO_2{}^+$. At the anharmonic level we, again, match the results of Mok *et al.* quite closely, although the geometry of $ClO_2{}^+$ that gives the best fit to experiment differs from theirs by 0.003 Å (1.411 Å versus 1.414 Å) in R_{Cl-O} (the predicted bond angle is the same in either case). Both geometries fall within the range of predictions made by the best post-Hartree-Fock *ab initio* treatments.[25] This fact, and the resulting close agreement

with experiment achieved for both calculations (ours and Mok *et al.*), makes it unlikely that the good results are an artifact of the geometric parameter adjustment.[52]

The full value of this new methodology will become more apparent when it is applied to larger species; something that we plan to do in the near future. The harmonic, first-order and second-order anharmonic calculations presented in this work required 0.09, 0.14, and 0.19 sec of CPU time, respectively, on an AMD XP 1900-Mhz computer. This computational efficiency is due in large part to the major truncation of the vibrational basis set. For ClO_2, using our algorithm to reduce the vibrational basis set, the number of states considered is only 55, 75, and 78 for the harmonic, first-order, and second-order terms, respectively. In order to obtain the same accuracy without truncation of the basis set the number of states needed is several thousand. Our method scales as M^3 where M is the number of vibrational states taken into account. Without truncation this number would grow much too rapidly for the method to be practical except for very small molecules. In the case of C_2H_4, which we are currently investigating, about 2×10^7 vibrational states would be needed for 1% accuracy, but with our truncation scheme this is reduced to less than 4×10^3 states.

Refinements of the algorithm and code currently being implemented add to our confidence that the methodology presented here will be adequate to simulate the spectra of much larger systems. We plan to take advantage of our program to calculate the vibrational contribution to two-photon absorption (TPA) of polyatomic molecules. This requires

evaluating transition dipole moment matrix elements for the entire vibrational manifold associated with a pair of electronic states, which may be done using the FCF's and the transition dipole moment surface as we have previously shown.[32] The same technique can be applied to obtain the Herzberg–Teller contributions to one-photon spectra.

ACKNOWLEDGMENTS

[1] F.-T. Chau, J. M. Dyke, E. P.-F. Lee, and D.-C. Wang, J. Electron Spectrosc. Relat. Phenom. **97**, 33 (1998).

[2] T. E. Sharp and H. M. Rosenstock, J. Chem. Phys. **41**, 3453 (1964).

[3] E. Hutchisson, Phys. Rev. **36**, 410 (1930).

[4] P. Chen, in *Unimolecular and Bimolecular Reaction Dynamics*, edited by C.-Y. Ng, T. Baer, and I. Powis (Wiley, Chichester, 1994), p. 371.

[5] K. M. Ervin, T. M. Ramond, G. E. Davico, R. L. Schwartz, S. M. Casey, and W. C. Lineberger, J. Phys. Chem. A **105**, 10822 (2001).

[6] H. Kikuchi, M. Kubo, N. Watanabe, and H. Suzuki, J. Chem. Phys. **119**, 729 (2003).

[7] P. T. Ruhoff, Chem. Phys. **186**, 355 (1994).

[8] J. Lermé, Chem. Phys. **145**, 67 (1990).

[9] R. Islampour, M. Dehestani, and S. H. Lin, J. Mol. Spectrosc. **194**, 179 (1999).

[10] E. V. Doctorov, I. A. Malkin, and V. I. Man'ko, J. Mol. Spectrosc. **64**, 302 (1977).

[11] P. R. Callis, J. T. Vivian, and L. S. Slater, Chem. Phys. Lett. **244**, 53 (1995).

[12] S. Schumm, M. Gerhards, and K. Kleinermanns, J. Phys. Chem. A **104**, 10648 (2000).

[13] D. Gruner, A. Nguyen, and P. Brumer, J. Chem. Phys. **101**, 10 366 (1994).

[14] R. Berger, C. Fischer, and M. Klessinger, J. Phys. Chem. A **102**, 7157 (1998).

[15] T. R. Faulkner and F. S. Richardson, J. Chem. Phys. **70**, 1201 (1979).

[16] F. Duschinsky, Acta Physicochim. URSS **7**, 551 (1937).

[17] K. C. Kulander, J. Chem. Phys. **71**, 2736 (1979).

[18] T. R. Faulkner and F. S. Richardson, J. Chem. Phys. **71**, 2737 (1979).

[19] P.-Å. Malmqvist and N. Forsberg, Chem. Phys. **228**, 227 (1998).

[20] B. Segev and E. J. Heller, J. Chem. Phys. **112**, 4004 (2000).

[21] S. Kallush, B. Segev, A. V. Sergeev, and E. J. Heller, J. Phys. Chem. A **106**, 6006 (2002).

[22] F. Iachello and S. Oss, Phys. Rev. Lett. **66**, 2976 (1991).

[23] T. Muller, P. H. Vaccaro, F. Perez-Bernal, and F. Iachello, J. Chem. Phys. **111**, 5038 (1999).

[24] H. Ishikawa, H. Toyosaki, N. Mikani, F. Pérez-Bernal, P. H. Vaccaro, and F. Iachello, Chem. Phys. Lett. **365**, 57 (2002).

[25] D. K. W. Mok, E. P. F. Lee, F.-T. Chau, D. Wang, and J. M. Dyke, J. Chem. Phys. **113**, 5791 (2000).

[26] P. Botschwina, B. Schulz, M. Horn, and M. Matuschewski, Chem. Phys. **190**, 345 (1995).

[27] K. Takeshita and N. Shida, Chem. Phys. **210**, 461 (1996).

[28] L. Serrano-Andrés, N. Forsberg, and P.-Å. Malmqvist, J. Chem. Phys. **108**, 7202 (1998).

[29] G. Barinova, N. Markovic, and G. Nyman, J. Chem. Phys. **111**, 6705 (1999).

[30] R. Neumann and C. Engler, Chem. Phys. **161**, 229 (1992).

[31] J. R. Reimers, J. Chem. Phys. **115**, 9103 (2001).

[32] D. M. Bishop, J. M. Luis, and B. Kirtman, J. Chem. Phys. **116**, 9729 (2002).

[33] D. M. Bishop and B. Kirtman, J. Chem. Phys. **95**, 2646 (1991).

[34] D. M. Bishop, J. M. Luis, and B. Kirtman, J. Chem. Phys. **108**, 10013 (1998).

[35] D. M. Bishop, Adv. Chem. Phys. **104**, 1 (1998).

[36] B. Kirtman, B. Champagne, and J. M. Luis, J. Comput. Chem. **21**, 1572 (2000).

[37] M. Torrent-Succarat, M. Sola, M. Duran, J. M. Luis, and B. Kirtman, J. Chem. Phys. **116**, 5363 (2002).

[38] P. Macak, Y. Luo, P. Norman, and H. Ågren, J. Chem. Phys. **113**, 705 (2000).

[39] P. Macak, Y. Luo, and H. Ågren, Chem. Phys. Lett. **330**, 447 (2000).

[40] A. Painelli, L. Del Freo, and F. Terenziana, Chem. Phys. Lett. **346**, 470 (2001).

[41] E. B. Wilson, Jr., J. C. Decius, and P. C. Cross, *Molecular Vibrations. The Theory of Infrared and Raman Vibrational Spectra* (Dover, New York, 1955).

[42] J. O. Hirschfelder, W. Byers Brown, and S. T. Epstein, Adv. Quantum Chem. **1**, 255 (1964).

[43] R. Flesch, E. Rühl, K. Hottmann, and H. Baumgärtel, J. Phys. Chem. **97**, 837 (1993).

[44] M. J. Frisch, G. W. Trucks, H. B. Schlegel *et al.*, Revision A.11, GAUSSIAN 98, Gaussian, Inc., Pittsburgh, 2001.

[45] K. A. Peterson and H.-J. Werner, J. Chem. Phys. **96**, 8948 (1992).

[46] K. A. Peterson and H.-J. Werner, J. Chem. Phys. **99**, 302 (1993).

[47] A. W. Richardson, R. W. Redding, and J. C. D. Brand, J. Mol. Spectrosc. **29**, 93 (1969).

[48] H. S. P. Muller, G. O. Sorenson, M. Birk, and R. R. Friedl, J. Mol. Spectrosc. **186**, 177 (1997).

[49] P. Chen, *Photoelectron Spectroscopy of Reactive Intermediates*, edited by C. Y. Ng, T. Baer, and I. Powis (Wiley, New York, 1994), Chap. 8, pp. 371–425.

[50] J. K. G. Watson, Mol. Phys. **15**, 479 (1968).

[51] J. K. G. Watson, Mol. Phys. **19**, 465 (1970).

[52] F.-T. Chau, J. M. Dyke, E. P. F. Lee, and K.-W. Mok, J. Chem. Phys. **118**, 4025 (2003).